SUPPLEMENTARY MATERIALS

Supplementary Figure 1. Representative wake EEG of *Grin2a* S644G/+ and wildtype +/+ littermates. No obvious epileptiform activity was observed in traces from at least seven *Grin2a*$^{S644G/+}$ mice recorded for 48 hours each.

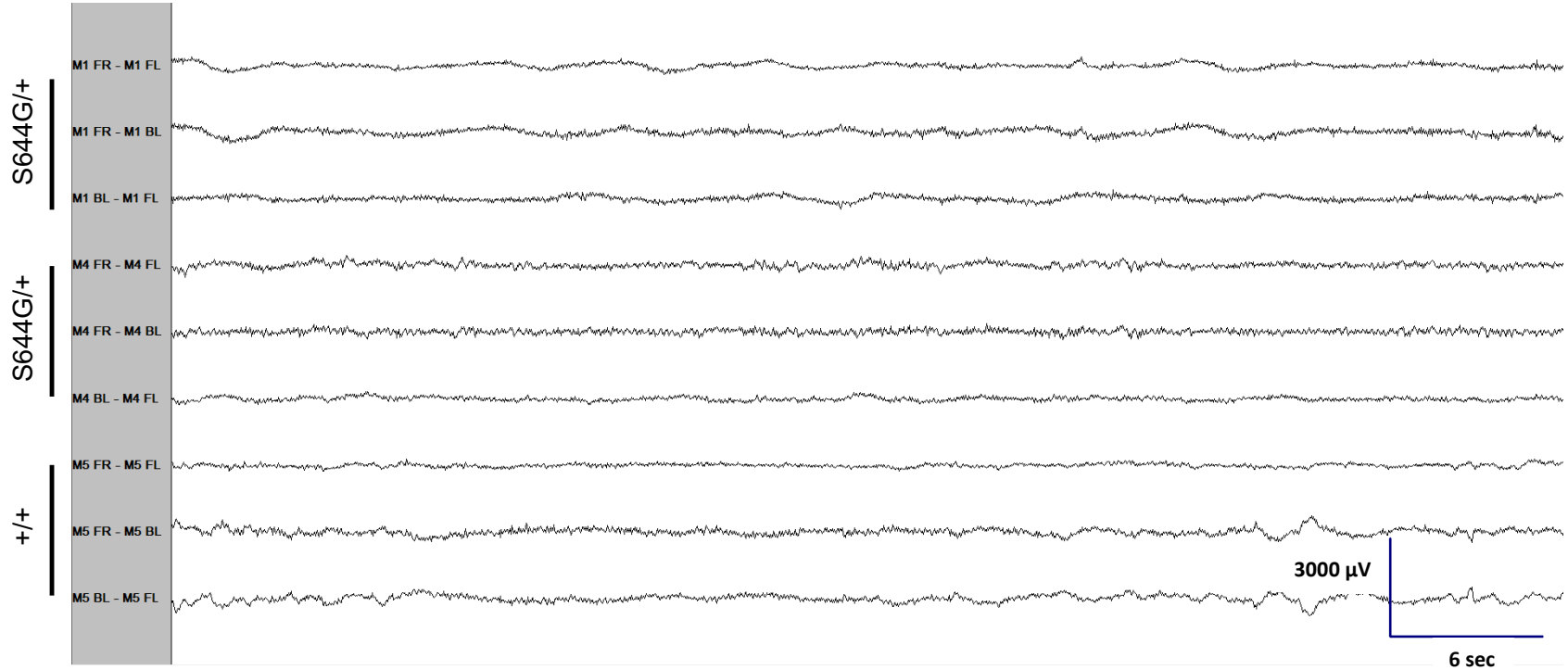

Supplementary Figure 2. Response of S644G-containing NMDARs to agonists *in vitro.* (a, b) Fitted composite glutamate and glycine concentration-response curves for diheteromeric human wildtype GluN1/GluN2A- and GluN1/GluN2A-S644G expressed in *Xenopus laevis* oocytes. Two-electrode voltage-clamp recordings were conducted at a holding potential of −40 mV. Glutamate potency was quantified as the half-maximally effective response (EC_{50}) of recombinant NMDARs receptors comprised of wild type or mutant GluNR2A in the presence of a maximally effective concentration of glycine (100 μM). Glycine potency was evaluated in the presence of a maximally effective concentration of glutamate (100 μM). (c, d) Fitted concentration-response curves for endogenous antagonists, Mg^{2+} (at -60 mV) and Zn^{2+}(at -20 mV) at diheteromeric human GluN1/GluN2A NMDARs. (e) Percentage current response at pH 6.8 versus 7.6 shows decreased current attenuation in the presence of increased proton concentrations. Concentration-response curves were generated for co-agonists glutamate and glycine, channel blocker Mg^{2+} and endogenous antagonist Zn^{2+} to evaluate whether the mutation changes agonist potency or the sensitivity to endogenous modulators. (f) Agonist potency shifts by GluN2A-S644G-containing NMDARs *in vitro*. Fitted concentration-response curves for glutamate, in the presence of 100 μM glycine (a), and glycine in the presence of 100 μM glutamate (g for NMDARs with 0, 1, or 2 copies of the rat GluN2A-S644G variant in *Xenopus laevis* oocytes. Results are mean ± SEM from 12-17 (glutamate) or 13-14 oocytes (glycine) from 2 separate injections. Either 1 or 2 copies of GluN2A-S644G significantly increases both glutamate and glycine potency of NMDA receptors ($p<0.05$, ANOVA, Neuman-Kuels multiple comparison test).

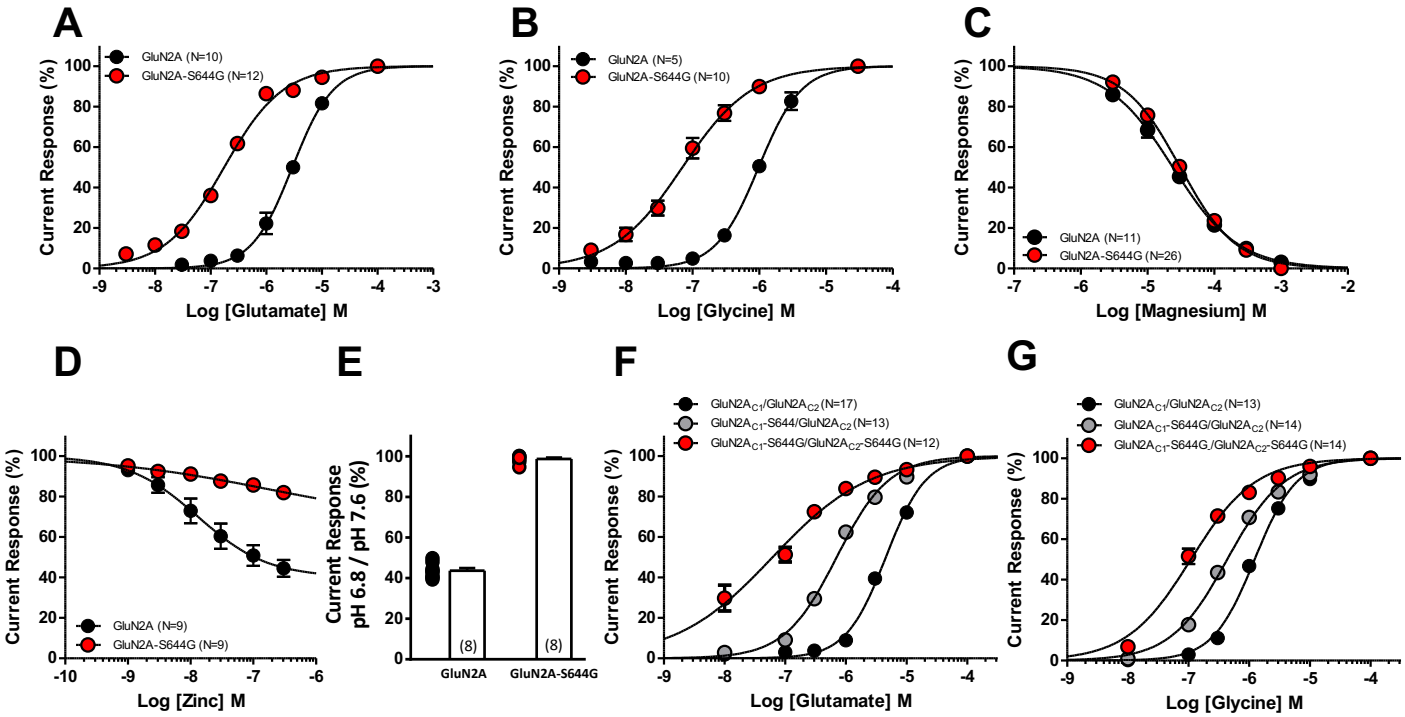

Supplementary Figure 3. Additional multielectrode array analyses. (a) Temporal development of number of active electrodes (electrodes recording at least 5 spikes per minute) shows >94% active electrodes for each genotype by DIV13. (b) Mutant networks displayed significantly longer network bursts (NB) relative to wildtype. Error bars in (a) and (b) indicate SEM – statistical tests were done as in Figure 6 and results listed on Supplementary Table 4. (c) Concentration-response curve of NMDA demonstrates sensitivity of mutant networks to NMDA-mediated excitation. Data for each well are normalized to the baseline firing recorded prior to agonist addition. Data were derived from 4 independent cultures with ≥ 17 wells for each genotype. (d) Peristimulus time histograms (400 ms) (see Materials and Methods) pre- and post-exposure to specified NMDA concentrations (n=6 wells). At baseline, mutant networks display prolonged evoked burst duration compared to wildtype with a mean AUC of 450 ± 10.7 compared to 330 ± 4.9 for wildtype. NMDA addition decreased evoked burst duration for both wildtype and mutant neurons in a concentration-dependent fashion. 1 µM NMDA; wildtype AUC 300 ± 5.4, S644G/S644G AUC 340 ± 8.8. 10 µM NMDA; wildtype AUC 250 ± 6.2 and S644G/S644G 140 ± 4.7.

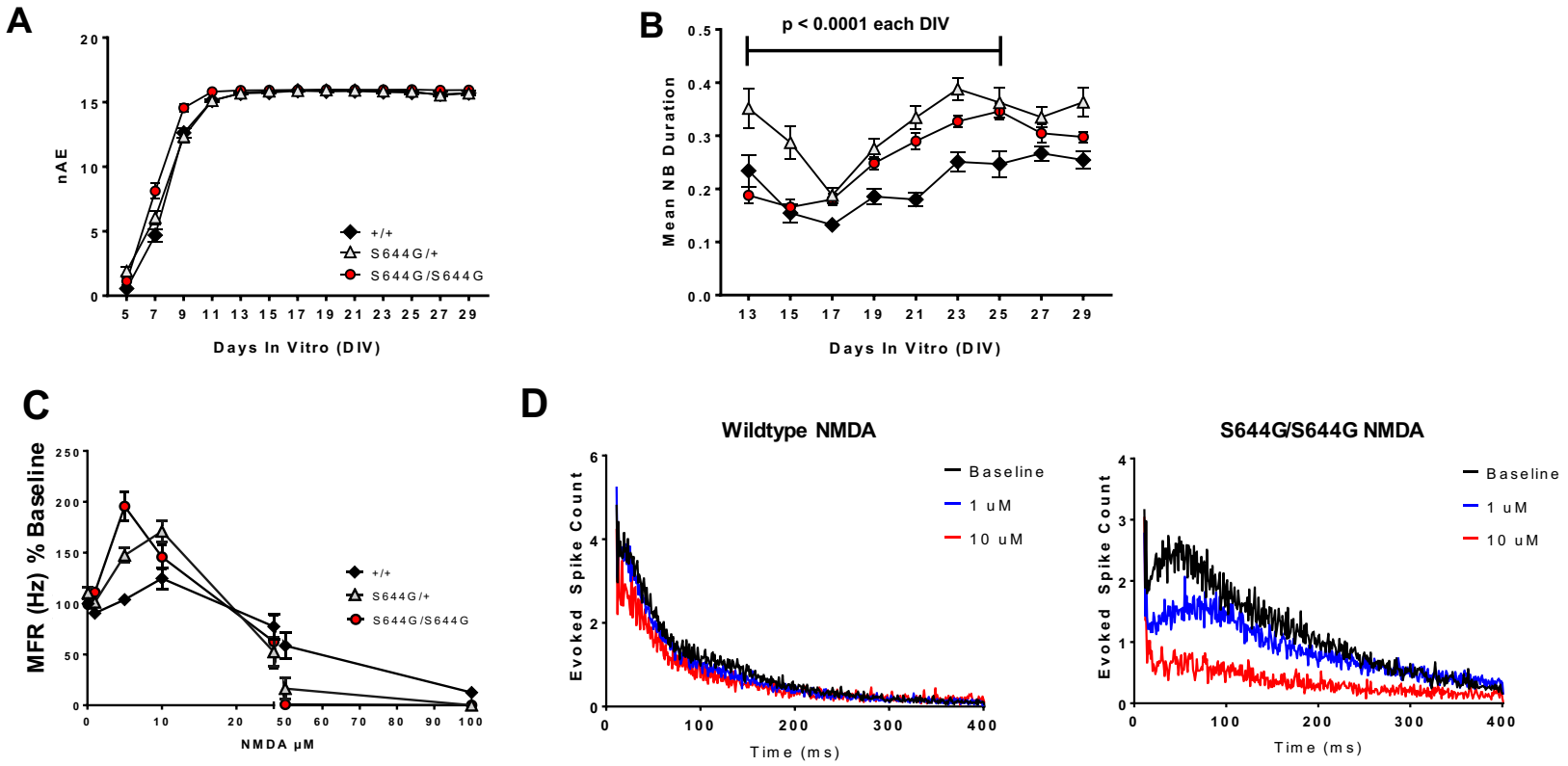

Supplementary Figure 4. Western blot of whole brain lysates probed for GluN2B, GluN2A, PSD95, β3-tubulin (N=3)**.** Uncropped images corresponding ot those shown in Figure 1d. (a) GRIN2B, (B) GRIN2A, (c) PSD95, (d) β-tubulin. Biological replicates (separate mice) are shown as 1, 2, 3.

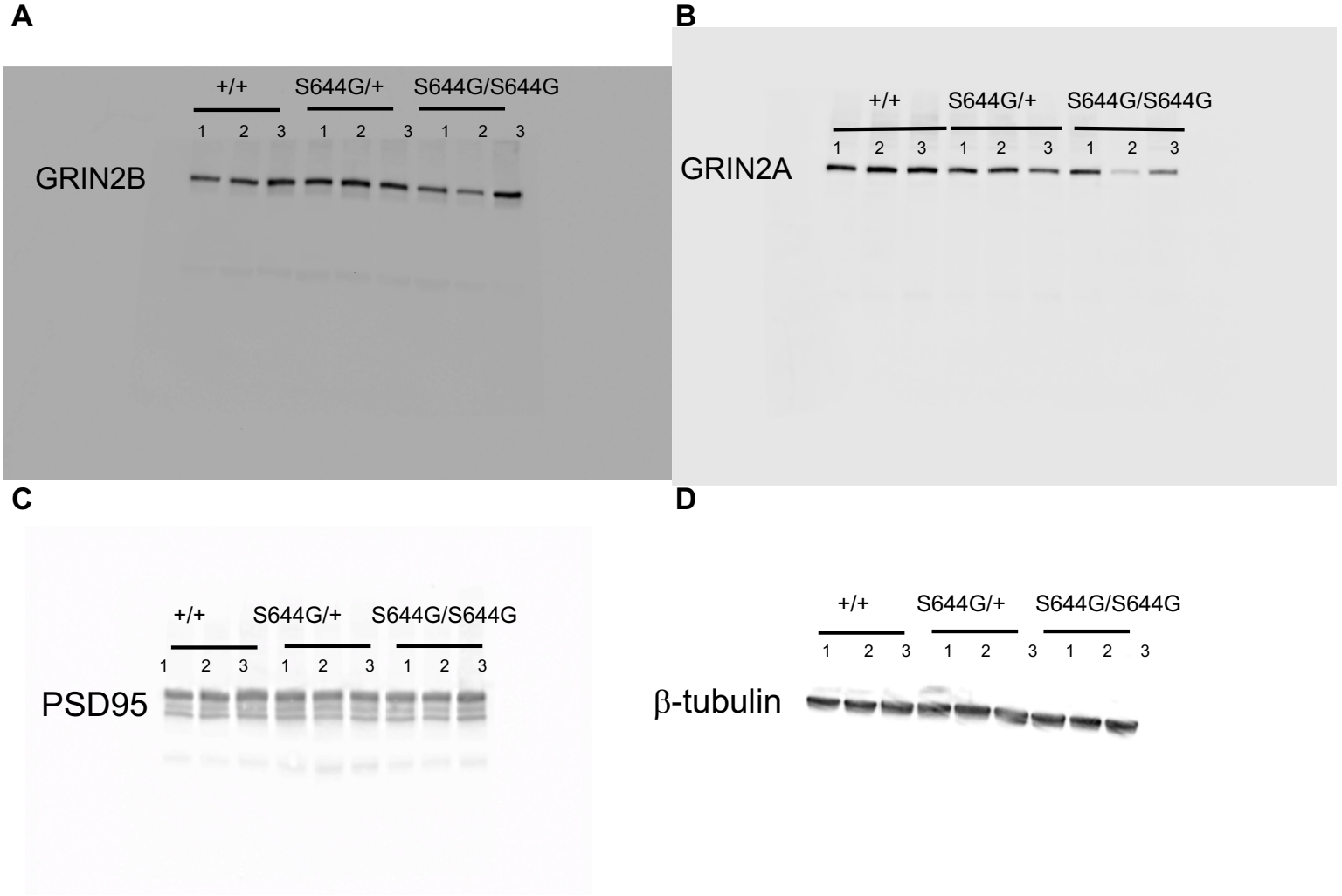

Supplementary Table 1. Pharmacological and functional properties of NMDARs containing GluN2A-S644G subunits

TEVC, oocytes	**GluN1/GluN2A$_{C1}$/GluN2A$_{C2}$**	**GluN1/GluN2A$_{C1}$-S644G/GluN2A$_{C2}$**	**GluN1/GluN2A$_{C1}$-S644G/GluN2A$_{C2}$-S644G**
Glu EC$_{50}$	4.5 μM (17; 4.0, 5.1)	0.71 μM (13; 0.58, 0.88)^	0.046 μM (12; 0.017, 0.12)^
Gly EC$_{50}$	1.2 μM (13; 1.0,1.5)	0.44 μM (14; 0.32, 0.61)^	0.11μM (14; 0.0081, 0.15)^
Dextromethorphan IC$_{50}$	13 μM (10; 11, 16)	25 μM (11; 20, 29)^	22 μM (13; 19, 25)^
Memantine IC$_{50}$	4.4 μM (20; 3.0, 6.6)	24 μM (10; 18, 34)^	30 μM (11; 20, 44)^
Patch clamp, HEK cells	**GluN1/GluN2A$_{C1}$/GluN2A$_{C2}$**	**GluN1/GluN2A$_{C1}$-S644G/GluN2A$_{C2}$**	**GluN1/GluN2A$_{C1}$-S644G/GluN2A$_{C2}$-S644G**
Amplitude (peak)	57 ± 21 pA/pF	22 ± 5 pA/pF	36 ± 16 pA/pF
Rise time	9.9 ± 2.0 ms	9.0 ± 1.4 ms	8.8 ± 1.5 ms
t_{FAST} deactivation	55 ± 4.6 ms	231 ± 38 ms	547 ± 156 ms
t_{SLOW} deactivation	--	1040 ± 253 ms	2130 ± 415 ms
t_{FAST} amplitude	100 %	72	66 %
t_W	55 ± 4.6 ms	456 ± 84*	1220 ± 264*, #
Charge transfer	2550 ± 691 pA ms/pF	10250 ± 3120* pA ms/pF	31000 ± 13100* pA ms/pF
n	14	8	9
MEA, cultured neurons	**WT**	**S644G/+**	**S644G/+**
Memantine IC$_{50}$	4.5 μM (29; 3.9, 5.2)	3.4 μM (46; 2.9, 3.9)	2.1 μM (4; 1.5, 2.8)*
Dextromethorphan IC$_{50}$	2.4 μM (26; 1.9, 2.8)	3.0 μM (27; 2.5, 3.6)	5.5 μM (12; 4.1, 6.6)*

Potency data for receptors with the indicated subunits are expressed as mean (n; 95% CI determined from log EC_{50} and IC_{50} values). ^ = non-overlapping confidence intervals. Functional data are mean ± SEM. -- indicates not detected, *=p<0.05 by one-way ANOVA for log (tau weighted, $\mathbf{t_W}$) and charge transfer compared to WT/WT; #=p<0.05 by one-way ANOVA for $\mathbf{t_W}$ compared to S644G/WT, Tukey's post-hoc analysis. Power to detect an effect size of 3 (e.g. a 2-fold change) was 0.99 for $\mathbf{t_W}$ and 1.5 for charge transfer was 0.98 (G*Power 3.0.10)

Supplementary Table 2. Statistical analyses of MEA activity phenotypes

	Firing Rate				Bursts per minute			
	Plate effect	Genotype effect			Plate	Genotype		
DIV	*p* -val	*p* -val	*p* -val adj.†	vs. wt^	raw only	*p* -val	*p* -val adj.†	vs. wt^
DIV9	9.29E-30	6.02E-02	ns		3.34E-25	3.75E-06	4.12E-05	hom
DIV11	3.86E-19	8.06E-05	8.86E-04	hom het	6.92E-20	1.26E-05	1.38E-04	hom
DIV13	4.65E-19	1.98E-09	2.18E-08	hom het	7.10E-19	2.08E-11	2.29E-10	hom het
DIV15	1.40E-20	3.83E-10	4.21E-09	hom het	4.89E-16	1.39E-12	1.53E-11	hom het
DIV17	2.94E-27	3.63E-09	3.99E-08	hom het	8.88E-10	1.68E-11	1.85E-10	hom het
DIV19	6.34E-11	7.33E-10	8.06E-09	hom het	1.10E-07	1.23E-08	1.35E-07	hom het
DIV21	5.50E-24	1.75E-06	1.93E-05	hom het	6.57E-21	3.33E-11	3.66E-10	hom het
DIV23	5.92E-15	6.63E-02	ns		1.79E-07	9.88E-11	1.09E-09	hom het
DIV25	1.93E-06	1.11E-01	ns		4.20E-09	1.84E-07	2.02E-06	hom het
DIV27	9.75E-08	1.41E-03	1.55E-02	hom	6.79E-10	4.74E-03	ns	
DIV29	1.53E-02	4.43E-01	ns		1.29E-04	7.23E-01	ns	

	Mutual Information				Network Burst Duration			
	Plate effect	Genotype effect			Plate	Genotype		
DIV	*p* -val	*p* -val	*p* -val adj.†	vs. wt^	raw only	*p* -val	*p* -val adj.†	vs. wt^
DIV9	1.46E-17	1.78E-12	1.96E-11	hom	9.07E-26	9.74E-01	ns	
DIV11	6.47E-14	2.89E-17	3.18E-16	hom	1.00E-23	1.54E-01	ns	
DIV13	3.27E-09	2.60E-23	2.86E-22	hom	3.75E-10	1.31E-07	1.44E-06	hom het
DIV15	5.20E-14	5.98E-11	6.58E-10	hom	7.31E-05	3.71E-09	4.08E-08	hom het
DIV17	2.54E-06	5.09E-11	5.60E-10	hom	1.27E-06	6.33E-09	6.96E-08	hom het
DIV19	2.02E-15	5.57E-05	6.12E-04	hom	1.62E-12	5.81E-10	6.39E-09	hom het
DIV21	1.47E-08	4.50E-05	4.95E-04	hom	5.35E-06	1.38E-18	1.52E-17	hom het
DIV23	1.99E-12	4.00E-05	4.40E-04	hom	4.29E-09	6.18E-13	6.80E-12	hom het
DIV25	2.54E-08	5.01E-01	ns		2.17E-13	5.34E-07	5.88E-06	hom het
DIV27	4.51E-10	4.14E-02	ns		3.89E-07	1.23E-03	1.35E-02	hom het
DIV29	1.44E-09	7.93E-04	8.72E-03	hom	8.05E-08	4.15E-04	4.57E-03	hom het

†Bonferroni adjustment: *p* -value x 11 (number of DIV's evaluated for each feature)
^Post-hoc Dunnet's test for hom vs wt or het vs wt, *p* <0.05